Intrinsic Magnetoresistance of Single-Walled Carbon Nanotubes Probed by a Noncontact Method

Yugo Oshima,[1,*] Taishi Takenobu,[1] Kazuhiro Yanagi,[2,3] Yasumitsu Miyata,[2] Hiromichi Kataura,[2,3] Kenji Hata,[4] Yoshihiro Iwasa,[1] and Hiroyuki Nojiri[1]

[1]*Institute for Materials Research, Tohoku University, Katahira 2-1-1, Sendai, 980-8577, Japan*
[2]*Nanotechnology Research Institute (NRI), National Institute of Advanced Industrial Science and Technology (AIST), 1-1-1 Higashi, Tsukuba 305-8562, Japan*
[3]*CREST, Japan Science and Technology Agency (JST), Honcho 4-1-8, Kawaguchi 332-0012, Japan*
[4]*Research Center for Advanced Carbon Materials, National Institute of Advanced Industrial Science and Technology (AIST), 1-1-1 Higashi, Tsukuba 305-8562, Japan*

(Received 26 May 2009; published 6 January 2010)

The intrinsic magnetotransport effect of the single-walled carbon nanotube (SWNT) has been observed by the cavity perturbation technique, which is a noncontact method for evaluating transport properties. The inverse Q factor of the cavity resonator, which corresponds to the resistance of the sample, shows a linear increase as a function of the magnetic field. The angular and tube diameter dependence of oriented SWNT thin films, and measurements using sorted SWNTs reveal that the observed positive magnetoresistance is due to the Aharonov-Bohm effect of metallic nanotubes.

DOI: 10.1103/PhysRevLett.104.016803 PACS numbers: 73.63.Fg, 75.47.Pq, 78.67.Ch

A single-walled carbon nanotube (SWNT), which is a seamless graphene cylinder with a nanoscale diameter and a micrometer-sized length, has attracted considerable interest because of its outstanding material properties and quantum effects. The electronic structure of the SWNT is determined by a band structure of the graphene sheet and periodic boundary conditions of the wave functions along the tube's circumference. For this reason, structural differences in the SWNTs, such as diameter or helical arrangement, yield remarkable differences in electronic and optical properties [1,2].

For instance, one-third of all possible SWNTs exhibit metallic properties for their gapless band structure. On the other hand, the remaining two-thirds behave as semiconductors, since they have a finite band gap of $E_g = 4\pi\gamma_b/3L$, where γ_b and L are the band parameters and the tube's circumference, respectively [Fig. 1(a)] [1,2].

Another fascinating feature of the SWNT is the magnetic field effect. When a field is applied parallel to the tube, the quantum states and dynamics of the electrons on the circumference are influenced by the so-called Aharonov-Bohm (AB) phase [3]. In such a case, the periodic boundary condition along the tube's circumference explicitly depends on the magnetic flux ϕ, and the band gap varies linearly as a function of the magnetic field, as shown in Fig. 1(b) [1,2]. These effects, referred to as the AB effect of the SWNTs, are among the unique properties of the SWNT. Indeed, the degeneracy lifting of E_g, which is due to the AB effect of the semiconducting tubes, has been observed by optical absorption [4,5]. In magnetotransport measurements, related behaviors are observed in multiwall carbon nanotubes as well [6–9].

Although some magnetotransport properties for single SWNT have been reported, their origins are still controversial [5,10,11]. One of the reasons for the unsuccessful observation of the AB effect of metallic SWNTs derives from the huge contact resistance. Meanwhile, for "multiple" SWNTs, some magnetotransport measurements have been performed on SWNT bundles and thin films, but only extrinsic effects have been observed [12–15].

SWNT bundles show negative magnetoresistance which can be explained by the weak localization effect [12,13]. Nonoriented SWNT thin films also show a weak localization effect in the low-field region, while positive magnetoresistance followed by the saturation of the resistance is observed for higher magnetic fields [14,15]. This behavior in the higher field region is attributed to spin-dependent

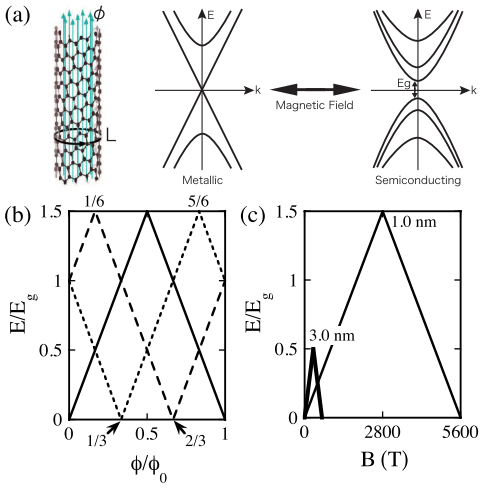

FIG. 1 (color online). (a) Schematic drawings of the SWNT and the typical energy dispersions of metallic and semiconducting SWNTs. (b) The predicted magnetic flux dependence of the energy gap [2]. The solid and broken lines are for metallic and semiconducting nanotubes, respectively. (c) The magnetic field dependence of the energy gap for metallic nanotubes with 1 and 3 nm diameters (thin and thick solid lines, respectively).

 © 2010 The American Physical Society

variable range hopping conduction [16]. These effects are considered to be due to the low dimensionality and the network effect of the spaghetti junctions of the SWNTs.

To exclude these extrinsic effects and observe the intrinsic magnetotransport properties, such as the AB effect, we have employed the following three techniques. First, a highly oriented SWNT thin film was prepared to study the true magnetic field effect along the tube's direction. The SWNT film was synthesized by mixing dispersed SWNTs in a melted polymer and then oriented by mechanical stretching [17]. 90% of the nanotubes were oriented within $\pm 15°$ of the stretched direction. Furthermore, the concentration of SWNTs was as low as 0.5 wt % of the substrate to minimize the extrinsic magnetic field effect attributed to contact between tubes. Second, we used cavity perturbation techniques, which are noncontact methods for evaluating transport properties. The cavity resonator has a particular resonant spectrum, which is described by the resonant frequency f and the quality factor Q, according to the size and the medium inside the cavity. The environment of the cavity is disturbed by the sample insertion, and f and Q changes in accordance with the permittivity or conductivity of the introduced sample. Thus, high-frequency conductivity of the SWNT can be obtained by comparing Q and f of the cavity with or without the sample [18]. There is no contact resistance issue since no electrode is needed for this technique. Finally, since synthesized SWNTs are a mixture of metallic and semiconducting nanotubes, all measurements were performed at 4.2 K, which is well below the gap of the semiconducting SWNT (i.e., $\sim$1 eV), to suppress the contribution of the semiconducting nanotubes. In principle, genuine magnetotransport effects of the metallic SWNT should be observed using this combination of methods.

In this Letter, we will present our noncontact magnetotransport measurements of the highly oriented SWNT thin films at low temperatures, where significant positive magnetoresistance is observed when the magnetic field is applied along the tube axis. Tube diameter dependence, using two kinds of SWNTs, was also evaluated. Moreover, sorted semiconducting tubes, obtained by state-of-the-art technology, were also measured to confirm the origin of the magnetoresistance. The use of sorted SWNTs has enabled differentiation of the magnetic field effect of the metallic and semiconducting tubes. All of the results lead us to conclude that the observed positive magnetoresistance is ascribed to the AB effect of metallic SWNTs.

The noncontact measurements were performed at IMR Tohoku University. A cylindrical cavity with the resonant frequency around 6.3 GHz was used in this study. At first, an empty cavity was measured at 4.2 K. The resonant frequency f_0 and the inverse Q factor $1/2Q_0$ were measured up to 14 T using a conventional superconducting magnet. Then, the sample was introduced into the cavity so that the oscillatory E field was applied parallel to the aligned direction. The resonant frequency f_s and the inverse Q factor $1/2Q_s$ were measured under the same condition.

Figure 2 shows the field dependence of the resonant frequency Δf $(=f_s - f_0)$ and the inverse Q factor $1/2\Delta Q$ $(=1/2Q_s - 1/2Q_0)$ for the highly oriented SWNT thin film at 4.2 K. The tubes used in the thin film were grown by the HiPco (high-pressure CO conversion) method, where the tube diameter was about 0.95 nm on average. The magnetic field was applied parallel and perpendicular to the tube axis. Each result is shown as an open circle and cross symbol, respectively. Considering the skin depth and the size of the sample, the microwave penetrated uniformly throughout the sample. In this case, the results should be treated by the so-called depolarization limit [18]. In Fig. 2, both Δf and $1/2\Delta Q$ increase as a function of the magnetic field. This indicates that the sample is on the metallic side of the depolarization regime, where $1/2\Delta Q$ is proportional to the resistance of the sample [18].

Although the magnetoresistance (i.e., $1/2\Delta Q$) is not so apparent for $B \perp$ tube, significant positive magnetoresistance is observed for $B \parallel$ tube. No saturation in the magnetoresistance was observed up to 14 T unlike previous results in nonoriented SWNT films, which showed a positive magnetoresistance and saturation at high magnetic fields [14,15]. The bare polyethylene thin film was measured beforehand, and the magnetic field effect of the polyethylene was verified to be negligible. Since the magnitude of the magnetoresistance strongly depends on the magnetic field orientation, it is likely that the positive magnetoresistance without saturation is an intrinsic magnetic field effects of the SWNT. Considering that 10% of

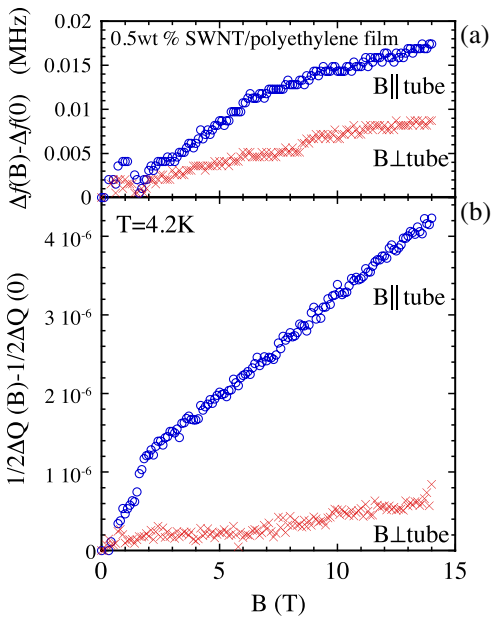

FIG. 2 (color online). The magnetic field dependence of Δf and $1/2\Delta Q$ of a highly oriented SWNT thin film at 4.2 K for $B \parallel$ tube and $B \perp$ tube. Each value is normalized with the value at zero field. The diameter of the SWNTs used in the thin film is about 0.95 nm (grown by HiPco methods).

the SWNTs are not aligned in the stretched direction, we think the small slope seen in $B \perp$ tube is due to the contribution of the misaligned tubes. The difference between the slopes agrees reasonably with this percentage.

Other oriented HiPco films showed similar linear increases in the magnetoresistance. The tangent of the slope was reproducible within an error of about 8%; this error likely derives from a small difference in the alignment or the diameter distribution of each film. Moreover, we have confirmed from Raman and absorption measurements that there is no doping effect from the surrounding matrix [17].

The AB effect depends on the magnetic flux penetrating the tube. As shown in Fig. 1(c), the quantum flux ϕ_0 corresponds to ~5600 T for a tube diameter of 1 nm. If the diameter were tripled to 3 nm, the magnetic field that corresponds to the quantum flux would be reduced by one-ninth (i.e. ~622 T). Since the energy gap E_g would also be reduced by one-third, the initial rising slope for the metallic nanotube with a 3 nm diameter would be expected to be 3 times larger than that of the 1 nm diameter, as shown in Fig. 1(c). Therefore, if we assume that the observed change in the magnetoresistance is related to the change in the energy gap, the slope of magnetoresistance should vary with the differences in the tube's diameter.

Hence, we have prepared a highly oriented thin film with 0.5 wt% SWNTs that are grown by the supergrowth method, where a diameter of a few nanometers can be obtained [19]. Although the diameter distribution is relatively large (e.g. 1–3 nm) compared with the HiPco tubes (± 0.11 nm), the supergrowth tube is a good candidate for observing the differences in magnetoresistance.

Figure 3 shows the magnetic field dependence of the $1/2\Delta Q$ for the highly oriented SWNT thin film of different tube diameters. The raw data of $1/2\Delta Q$ are proportional to the sample volume, and $1/2\Delta Q$ is normalized to the so-called size factor γ for comparison [18]. The size factor γ can be described as $\gamma = 2V_S/V_C$, where V_S and V_C are the volume of the sample and the cavity, respectively. The results of the SWNTs grown by HiPco and by the supergrowth method, which have a diameter of about 0.95 and 1–3 nm, respectively, are shown as circle and square symbols. The magnetic field is applied along the stretched direction. The size factor γ for the HiPco and supergrowth films is 46.3×10^{-6} and 43.8×10^{-6}, respectively.

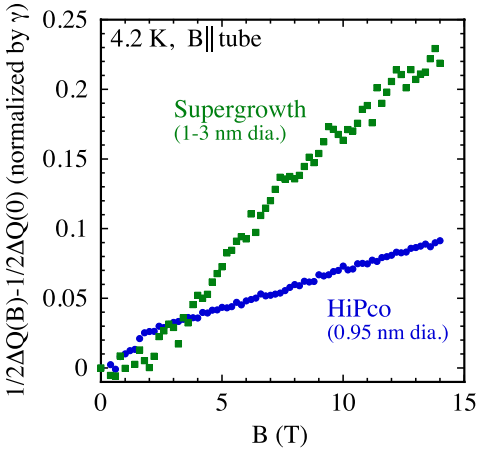

FIG. 3 (color online). The typical magnetic field dependence of the $1/2\Delta Q$ at 4.2 K for oriented thin film with SWNTs grown by HiPco (circle) and supergrowth (square) methods. The diameter of the tubes is 0.95 ± 0.11 nm and 1–3 nm, respectively. Each value is normalized to the value for the zero field and its size factor γ. The raw HiPco data are taken from Fig. 2.

As the results in Fig. 3 show, positive magnetoresistance without saturation is also observed for supergrowth SWNT thin film. Moreover, the slope for the supergrowth SWNTs is about 2.5 times larger than that of the HiPco SWNTs. In contrast to the HiPco films, which display quantitatively reproducible positive magnetoresistance, data for the supergrowth films are more sample dependent, possibly due to the large diameter distribution. However, the magnetoresistance of the supergrowth film falls in the range of 1.7 to 2.5 times larger than that of the HiPco film. Considering that the measurements are performed at 4.2 K, where the contribution of semiconducting tubes is minimal, these results clearly indicate that the observed magnetoresistance is due to the AB effect of the metallic tubes. Notably, the uncertainty of SWNTs' concentration (0.5 wt %) in each film is almost negligible with our fabrication method; therefore, the difference in the slopes comes mainly from the diameter [17].

So far, we have investigated SWNT samples, which are mixtures of metallic and semiconducting tubes. Recent progress in sorting SWNTs has made it possible to obtain high-quality semiconducting tubes, which offer a chance to verify whether the effect of the semiconducting tube is really suppressed at 4.2 K. Sorted semiconducting SWNTs were obtained by the density-gradient ultracentrifuge sorting technique [20,21]. The concentration of the semiconducting SWNT is estimated to be over 95% from a comparison of the integral intensities of S11, S22, and M11 absorption bands.

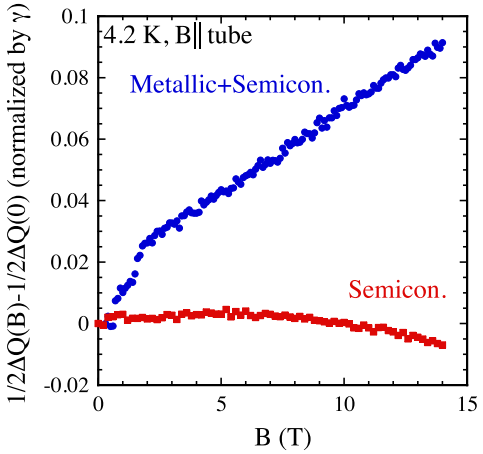

FIG. 4 (color online). Comparison of the $1/2\Delta Q(B) - 1/2\Delta Q(0)$ of oriented thin film with the mixed SWNTs (circle) and the semiconducting SWNTs (square) at 4.2 K.

Figure 4 is a comparison between the oriented thin film made from a mixture of the metallic and semiconducting SWNTs, and the pure semiconducting SWNTs. Both films have the same content rate (0.5 wt %); the diameter of the semiconducting tube is about 1.4 ± 0.1 nm. The magnetic field is applied to the stretched direction. The y axis is normalized by the size factor γ for comparison, where γ for the semiconducting film is 41.2×10^{-6}. As shown in Fig. 4, the magnetic field effect of the semiconducting SWNTs is minimally apparent when compared with the mixed SWNTs thin film. This implies that the magnetic field effect of the semiconducting tubes is largely suppressed at this temperature, and the positive magnetoresistance observed in Fig. 3 originates from the metallic nanotubes. In addition, the pure semiconducting tubes have the opposite effect of the metallic tubes (i.e., negative slope in Fig. 4), in a manner consistent with the behavior of the energy gap as a function of the magnetic flux in Fig. 1(b). Namely, the band gap closes in the semiconducting tubes, leading to a negative magnetoresistance. From the behavior observed in Fig. 4, and the angular and diameter dependence in Figs. 2(b) and 3, we conclude that the observed positive magnetoresistance arises from the AB effect of the metallic SWNTs.

In the metallic region of the depolarization regime, the relation between the change of the inverse Q factor and the resistivity can be described as $1/2\Delta Q = f_0\gamma\rho/2n^2$; ρ is the real part of the complex resistivity and n is the depolarization factor, and n can be obtained from the relation $\Delta f/f_0 \approx -\gamma/n$ in this regime [18]. However, a crucial error in Δf is always caused by the opening and closing of the cavity for sample introduction, and the absolute value of the resistivity ρ is difficult to obtain. On the other hand, the relative value, such as the magnetoresistance $\Delta\rho/\rho(0) = [\rho(B) - \rho(0)]/\rho(0)$, is readily obtained since the factor $2n^2/f_0\gamma$ can be neglected. Therefore, $\Delta\rho/\rho(0) = [1/2\Delta Q(B) - 1/2\Delta Q(0)]/1/2\Delta Q(0)$. For the result of the 0.95 nm tube in Fig. 2(b), the value of $1/2\Delta Q$ at zero field is 143×10^{-6}. This leads to a magnetoresistance of about 3% at 14 T for the ''oriented'' thin film, while $\Delta\rho/\rho(0)$ for the nonoriented thin film saturates at around 10%–20% due to the extrinsic effect mentioned above [14,15]. Therefore, it seems reasonable that the AB effect was never observed for nonoriented SWNT assemblies.

Meanwhile, the AB effect for metallic SWNTs should lead to a monotonic, but nonlinear increase in the resistivity up to half of ϕ_0 [22,23]. Considering that our maximum magnetic field corresponds to only $\phi_{\max}/\phi_0 \sim 0.0025$, we are observing only a tiny area of the full magnetotransport change of the AB effect. This is probably why we are observing only a linear increase in the magnetoresistance.

The origin of the hump structure, observed around 2 T in Fig. 2(b), still needs to be solved. While the hump does not always appear, some kinds of kink structures are usually observed around 2 T. Possibly, magnetic impurities, which are usually relevant for HiPco tubes, are the origin of the hump. However, effects of strain and curvature, which lead to magnetoconductivity peaks, are also possible since the kinks are also observed for supergrowth film in Fig. 3 [24].

To summarize, we have successfully observed the AB effect of metallic SWNT using a noncontact method. In contrast to the conventional transport measurements where only extrinsic effects were observed, our methods enable observation of the genuine magnetotransport properties of the SWNT, such as the AB effect. This technique is promising for future studies of SWNT.

This study has been supported in part by Industrial Technology Research Grant Program in 2006 from New Energy and Industrial Technology Development Organization (NEDO) of Japan, and in part by the Grant-in-Aid for Young Scientist (B) (No. 20740183) from the Ministry of Education, Culture, Sports, Science and Technology of Japan. This work has been performed at the High Field Laboratory for Superconducting Materials, Institute for Materials Research, Tohoku University.

*Present address: RIKEN, Hirosawa 2-1, Wako, 351-0198, Japan.
yugo@riken.jp

[1] H. Ajiki and T. Ando, J. Phys. Soc. Jpn. **62**, 1255 (1993).
[2] T. Ando, J. Phys. Soc. Jpn. **74**, 777 (2005).
[3] Y. Aharonov and D. Bohm, Phys. Rev. **115**, 485 (1959).
[4] S. Zaric *et al.*, Science **304**, 1129 (2004).
[5] J. Kono *et al.*, Top. Appl. Phys. **111**, 393 (2008).
[6] A. Bachtold *et al.*, Nature (London) **397**, 673 (1999).
[7] A. Fujiwara *et al.*, Phys. Rev. B **60**, 13492 (1999).
[8] U. C. Coskun *et al.*, Science **304**, 1132 (2004).
[9] B. Lassagne *et al.*, Phys. Rev. Lett. **98**, 176802 (2007).
[10] J. Vavro, J. M. Kikkawa, and J.E. Fischer, Phys. Rev. B **71**, 155410 (2005).
[11] G. Fedorov *et al.*, Nano Lett. **7**, 960 (2007).
[12] J. R. Kim *et al.*, Phys. Rev. B **66**, 233401 (2002).
[13] V. Krstić *et al.*, Synth. Met. **135–136**, 799 (2003).
[14] G. T. Kim *et al.*, Phys. Rev. B **58**, 16064 (1998).
[15] T. Takano *et al.*, J. Phys. Soc. Jpn. **77**, 124709 (2008).
[16] H. Kamimura *et al.*, Physica (Amsterdam) **117–118B+C**, 652 (1983).
[17] N. Akima *et al.*, Adv. Mater. **18**, 1166 (2006).
[18] O. Klein *et al.*, Int. J. Infrared Millim. Waves **14**, 2423 (1993).
[19] K. Hata *et al.*, Science **306**, 1362 (2004).
[20] M. S. Arnold *et al.*, Nature Nanotech. **1**, 60 (2006).
[21] K. Yanagi *et al.*, Appl. Phys. Express **1**, 034003 (2008).
[22] S. Roche and R. Saito, Phys. Rev. Lett. **87**, 246803 (2001).
[23] Z. Zhang *et al.*, Phys. Rev. B **66**, 085405 (2002).
[24] T. Nakanishi and T. Ando, J. Phys. Soc. Jpn. **74**, 3027 (2005).